

## Electronic Supplementary Information

### **A simple and rapid mix-and-read assay for sensitive detection of O6-methylguanine DNA methyltransferase**

Ming-hao Liu, ‡,<sup>a</sup> Wan-tong Yu, ‡,<sup>a</sup> Xiao-yun Yang, ‡,<sup>b</sup> Yueying Li, <sup>\*c</sup> Yan Zhang, <sup>\*a</sup> Chun-yang Zhang, <sup>\*a</sup>

<sup>a</sup> College of Chemistry, Chemical Engineering and Materials Science, Shandong Normal University, Jinan 250014, China.

<sup>b</sup> Department of Pathology, Affiliated Hospital of Guangdong Medical University, Zhanjiang, 524001, China.

<sup>c</sup> Institute of Immunity and Infectious Diseases, School of Medicine and Pharmaceutical Sciences, Zhengzhou University, Zhengzhou 450000, China.

\*Corresponding author. E-mail: cyzhang@sdu.edu.cn; yanzhang\_2003@163.com; liyueying1115@qq.com.

‡ These authors contributed equally.

## EXPERIMENTAL SECTION

### Chemicals and Materials

All HPLC-purified oligonucleotides (Table 1) were purchased from Accurate Biotechnology (Hunan) Co. Ltd. (Changsha, China). Human O<sup>6</sup>-methylguanine-DNA Methyltransferase (MGMT) was obtained from Cayman Chemical (Ann Arbor, MI, USA). PvuII, Exonuclease III (Exo III), Lambda Exonuclease ( $\lambda$  Exo), 10 × NEBuffer™ r3.1 (1 M NaCl, 500 mM Tris-HCl, 100 mM MgCl<sub>2</sub>, 1 mg/mL recombinant albumin, pH 7.9), 10 × NEBuffer™ 1 (100 mM Bis-Tris-Propane-HCl, 100 mM MgCl<sub>2</sub>, 10 mM DTT, pH 7) and 10 × Lambda Exonuclease Reaction Buffer (670 mM Glycine-KOH, 25 mM MgCl<sub>2</sub>, 500 μg/ml BSA, pH 9.4) were purchased from New England Biolabs Inc. (Beverly, MA, U.S.A.). O<sup>6</sup>-benzylguanine (O<sup>6</sup>-BG) was obtained from Sigma-Aldrich (MO, USA). Human MGMT enzyme-linked immunosorbent assay (ELISA) kit was purchased from Meimian Biotechnology (Yancheng, Jiangsu, China). All ultrapure water is prepared by a Millipore Milli-Q Water Purification System (Billerica, MA, USA).

**Table S1.** Sequences of the Oligonucleotides <sup>a</sup>

Oligonucleotide	Sequence (5'→3')
Dumbbell probe	TTC CTC GAT CTT GAT AGG GAG AAA AAA CAA GAT CGA GGA AGT CGC GCA <u>GCT</u> GCG AAA GAA GAA AGA CAG AAA TTT CGC AGC TGC GCG AC
Signal probe	BHQ3-AAG ATC GAG GAA GTC GC-Cy5

<sup>a</sup> The underlined “G” is O<sup>6</sup>-methylguanine (O<sup>6</sup>-MeG).

### Detection of MGMT activity

The reaction was performed in a 30  $\mu\text{L}$  of solution containing 150 nM dumbbell probe, 500 nM signal probe, 18 U of PvuII, 9 U of Exo III, 1 $\times$  NEBuffer<sup>TM</sup> r3.1 (100 mM NaCl, 50 mM Tris-HCl, 10 mM MgCl<sub>2</sub>, 100  $\mu\text{g}/\text{ml}$  recombinant albumin, pH 7.9), 1 $\times$  NEBuffer<sup>TM</sup> 1 (10 mM Bis-Tris-Propane-HCl, 10 mM MgCl<sub>2</sub> and 1 mM DTT, pH 7), and different concentrations of MGMT. The reaction mixture was incubated at 37  $^{\circ}\text{C}$  for 60 min. The amplification product was diluted to a final volume of 70  $\mu\text{L}$  for fluorescence measurements. The fluorescence emission spectrum of Cy5 was recorded by using a FLS1000 spectrophotometer (Edinburgh, UK) with an excitation wavelength of 620 nm. The fluorescence intensity at 662 nm was used for data analysis.

### **Gel electrophoresis**

Non-denaturing polyacrylamide gel electrophoresis (PAGE) was used to analyze the PvuII-mediated cleavage products and Exo III-mediated digestion products. The PvuII-mediated cleavage products were stained with fluorescent dyes SYBR Gold and analyzed by 8 % PAGE in 1 $\times$  TBE buffer (9 Mm Tris-HCl, 9 Mm boric acid, 0.2 mM EDTA, pH 7.9) at 110V for 35 min. The Exo III-mediated digestion products were analyzed by 8 % PAGE in 1 $\times$  TBE buffer at 110V for 30 min. Gel imaging was obtained by using a Bio-Rad ChemiDoc MP Imaging System (Hercules, CA).

### **Inhibition assay**

Different concentrations of inhibitors were added to 30  $\mu\text{L}$  of solution containing 0.01 ng/ $\mu\text{L}$  MGMT, 150 nM hairpin probe, 500 nM signal probe, 18 U of PvuII, 9 U of Exo III, 1 $\times$ NEBuffer<sup>TM</sup> r3.1 (100 mM NaCl, 50 mM Tris-HCl, 10 mM MgCl<sub>2</sub>, 100  $\mu\text{g}/\text{ml}$  recombinant albumin, pH 7.9), 1 $\times$  NEBuffer<sup>TM</sup> 1 (10 mM Bis-Tris-Propane-HCl, 10 mM MgCl<sub>2</sub> and 1 mM DTT, pH 7), and the solution was incubated at 37 $^{\circ}\text{C}$  for 60 min. The relative activity ( $RA$ ) of MGMT was calculated according to equation 1.

$$RA = \frac{C_i}{C_t} \times 100\% = 10^{(F_i - F_t)/5445} \times 100\% \quad (1)$$

where  $F_t$  is the Cy5 fluorescence intensity in the presence of MGMT, and  $F_i$  is the Cy5 fluorescence intensity in the presence of MGMT + inhibitors.  $C_t$  and  $C_i$  are calculated from the linear correlation equation (Fig. 2), respectively.

$$F_t = 49558 + 5445 \lg C_t \quad (2)$$

$$F_i = 49558 + 5445 \lg C_i \quad (3)$$

The half maximal inhibitory concentration ( $IC_{50}$ ) was calculated by fitting the curve of  $RA$  versus the inhibitor concentration.

### **Cell culture and cell extraction**

Human epidermoid carcinoma cells (A431 cells), human cervical cancer cell line (HeLa cells) and human breast adenocarcinoma cell line (MCF-7 cells) were purchased from Cell Bank of Chinese Academy of Sciences (Shanghai, China). A431 cells, HeLa cells and MCF-7 cells were grown in Dulbecco's modified Eagle's medium (DMEM, Gibco, USA) containing 10% fetal bovine serum (FBS) and 1% penicillin-streptomycin (PS) at 37 °C under a humidified atmosphere with 5% CO<sub>2</sub>. The cells growing in exponential growth phase were harvested by using trypsinization, PBS (pH 7.4) washing, and centrifugation at 800 rpm for 5 min at 4°C. Subsequently, the nuclear and cytoplasmic extracts were prepared using the nuclear extract kit (ActiveMotif, Carlsbad, CA, U.S.A.). The obtained extracts were stored at -80°C.

## **SUPPLEMENTARY RESULTS**

### **Mechanism of O<sup>6</sup>-MeG demethylation by MGMT**

The MGMT-initiated demethylation process of O<sup>6</sup>-MeG is shown in Fig. S1. MGMT is a suicide DNA repair enzyme that specifically removes alkyl adducts from O<sup>6</sup>-alkylated guanines to the cysteine residue

(Cys145) of MGMT by an irreversible bimolecular nucleophilic substitution reaction, leading to direct repair of G and inactivation of MGMT.<sup>1, 2</sup>

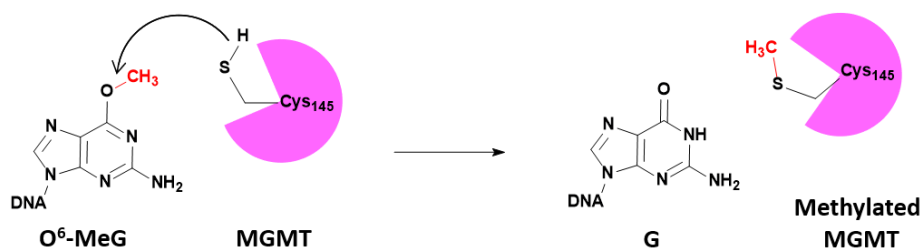


**Fig. S1** Mechanism of MGMT-initiated O<sup>6</sup>-MeG demethylation.

### Measurement of Cy5 fluorescence signal under different experimental conditions

Previous studies demonstrated that Exo III may slowly digest ssDNA.<sup>3, 4</sup> Therefore, we investigated the digestion activity of Exo III toward the single-stranded signal probe (SP). As shown in Fig. S2, we investigated the digestion of signal probes by Exo III under four experimental conditions including experimental group with MGMT (MGMT + dumbbell Probe + PvuII + Exo III + signal probe, red line), control group without MGMT (dumbbell Probe + PvuII + ExoIII + signal probe black line), Exo III experimental group (Exo III+ signal probe, blue line), and signal probe group (signal probe only, green line). A high Cy5 signal is detected in the presence of MGMT (red line), but an extremely low Cy5 signal is detected in the absence of MGMT (black line), which is consistent with Fig. 1 C. In addition, the Cy5 fluorescence intensity in Exo III experimental group (blue line) is identical to that in the control group (black line), indicating that the presence of dumbbell Probes and PvuII does not affect the digestion of signal probe by Exo III. Moreover, the Cy5 fluorescence signal in Exo III experimental group (blue line) is identical to that in signal probe group (green line), suggesting that Exo III can hardly digest single-stranded signal probe. Therefore, the Cy5 signal is generated only by MGMT.

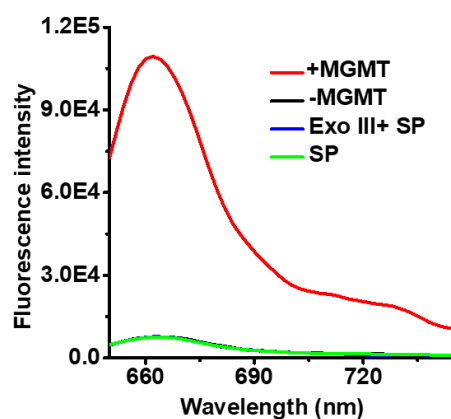


**Fig. S2** Measurement of Cy5 fluorescence signal under different experimental conditions. Red line, experimental group (MGMT + dumbbell Probe + PvuII + Exo III + signal probe); Black line, control group (dumbbell Probe + PvuII + Exo III + signal probe); Blue line, Exo III experimental group (Exo III+ signal probe); Green line, signal probe group (signal probe only). The 10 ng/ $\mu$ L MGMT, 150 nM dumbbell Probe, 0.6 U/ $\mu$ L PvuII, 0.3 U/ $\mu$ L ExoIII and 500 nM signal probe were used in this research.

### Comparison of the assay performance between using $\lambda$ Exo and using Exo III

Similar to Exo III, Lambda exonuclease ( $\lambda$  Exo) is a DNA exonuclease and has been widely used in nucleic acid signal amplification strategies.<sup>5, 6</sup>  $\lambda$  Exo uses double-stranded DNA as the substrate and selectively digests the 5-phosphorylated strand of dsDNA along 5'→3' direction. Since the product of the dumbbell probe cleaved by PvuII contains the 5-PO<sub>4</sub> end,  $\lambda$  Exo can cleave the PvuII product to achieve a one-step signal amplification (Fig. S3B). Thus, we compared the assay performance between using Exo III (Fig. S2A) and using  $\lambda$  Exo (Fig. S3B) under the identical experimental condition. The signal probe sequence for  $\lambda$  Exo is BHQ3-GCG AC TTC CTC GAT CTT -Cy5. The Cy5 fluorescence signal generated using Exo III (Fig. S3C) is much higher than that generated using  $\lambda$  Exo (Fig. S3D). In addition, the background signal generated using  $\lambda$  Exo (Fig. S3D, black line) is much higher than that generated using Exo III (Fig. S3C, black line). Thus, Exo III is used in the subsequent research.

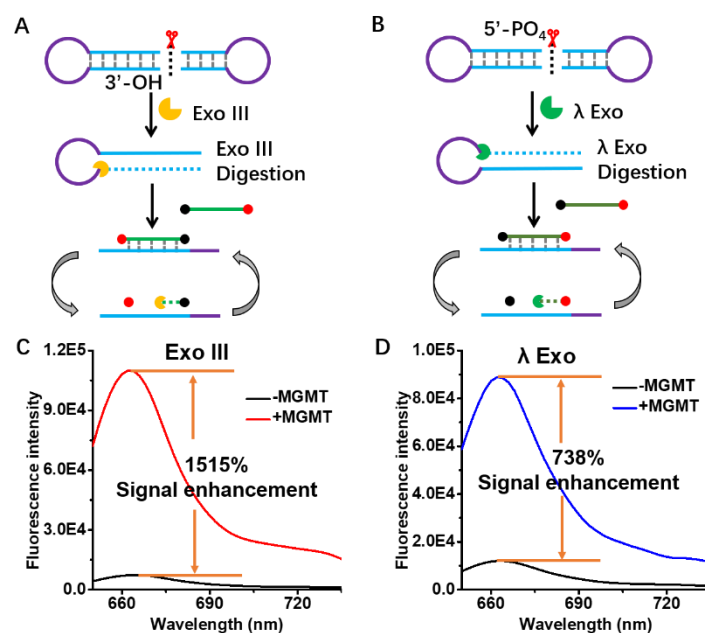


**Fig. S3** (A) Schematic illustration of Exo III -mediated signal amplification strategy. (B) Schematic illustration of  $\lambda$  Exo -mediated signal amplification strategy. (C) Fluorescence emission spectra produced by Exo III-mediated signal amplification strategy in the absence (black line) and presence (red line) of MGMT. (D) Fluorescence emission spectra produced by  $\lambda$  Exo-mediated signal amplification strategy in the absence (black line) and presence (blue line) of MGMT. The MGMT concentration is 10 ng/ $\mu$ L.

### Assessment of amplification efficiency

We evaluated the amplification efficiency of the proposed method. Since the signal amplification process of the proposed method is achieved by the digestion of signal probes catalyzed by Exo III, we calculated the concentration of the digested signal probes in the presence and absence of MGMT to assess the signal amplification efficiency. We first measured the Cy5 fluorescence signals generated by different concentrations of Cy5-abeled DNA probes (The sequence of Cy5 labeled DNA probes is AAG ATC GAG GAA GTC GC-Cy5) (Fig. S5 A) and signal probes (Fig. S5 B). The linear equation between Cy5 fluorescence intensity and the Cy5-labeled DNA probes concentration is  $F_{Cy5} = 450.94 C_{Cy5} + 28.71$  ( $R^2 =$

0.996), where  $C_{Cy5}$  is the concentration of Cy5-labeled DNA probes and  $F_{Cy5}$  is the measured Cy5 fluorescence intensity. The linear equation between Cy5 fluorescence intensity and the Cy5-labeled DNA probes concentration is  $F_{BHQ-Cy5} = 14.61 C_{BHQ-Cy5} + 26.35$  ( $R^2 = 0.995$ ), where  $C_{BHQ-Cy5}$  is the concentration of signal probe and  $F_{BHQ-Cy5}$  is the Cy5 fluorescence intensity produced by signal probes. Since the concentration of signal probe is fixed (500 nM), i.e.,  $C_{Cy5} + C_{BHQ-Cy5} = 500$  nM, we can calculate the concentration of Cy5 generated by Exo III-assisted signal amplification according to the following equations:

$$F = F_{Cy5} + F_{BHQ-Cy5} = 450.94 C_{Cy5} + 28.71 + 14.61 \times (500 - C_{Cy5}) + 26.35 \quad (4)$$

$$F = 436.33 C_{Cy5} + 7360.06 \quad (5)$$

By bringing the fluorescence intensity in the presence (109457.04) and absence (7545.77) of MGMT (Fig. S2) into equation 5, the concentration of produced Cy5 in the presence of MGMT is calculated to be 233.99 nM, and the concentration of Cy5 in the absence of MGMT is measured to be 0.42 nM.

To quantitatively evaluate the amplification reaction, the fold amplification is estimated based on equation 6.

$$\text{Fold amplification} = \frac{C_1}{C_0} \quad (6)$$

where  $C_1$  is the measured concentration of Cy5 (nM) in the presence of 10 ng/ $\mu$ L MGMT and  $C_0$  is the measured concentration of Cy5 (nM) in the absence of MGMT. When the MGMT concentration is 10 ng/ $\mu$ L, the amplification efficiency of the proposed method is 557-fold.



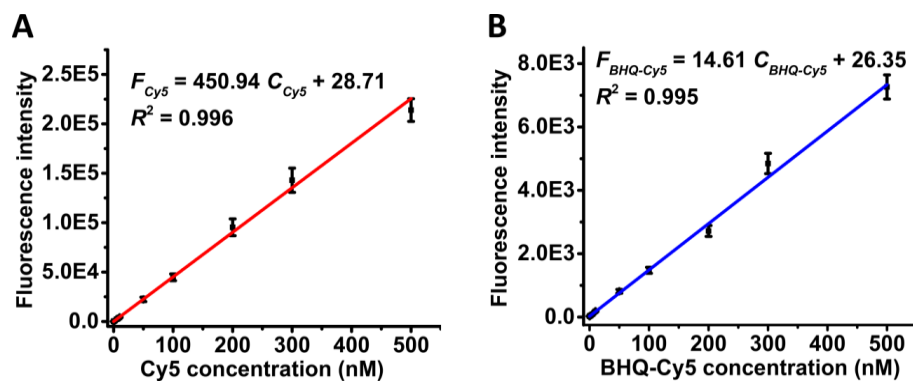


**Fig. S4** (A) Fluorescence intensity produced by different concentrations of Cy5. (B) Fluorescence intensity produced by different concentrations of BHQ-Cy5. Error bars represent the standard deviation of three experiments.

### Optimization of experimental conditions

To obtain the best assay performance, we evaluated the effect of Exo III concentration, PvuII concentration, dumbbell probe substrate concentration and reaction time upon the assay performance by monitoring the variation of  $F/F_0$  ( $F$  and  $F_0$  are the Cy5 fluorescence intensity in the presence of MGMT and absence of MGMT, respectively). As shown in Fig. S5A, the value of  $F/F_0$  improves with the increasing concentration of Exo III from 0.1 to 0.3 U/ $\mu$ L, followed by decrease beyond the concentration of 0.3 U/ $\mu$ L due to the background signal induced by the digestion of single-stranded signal probes by high-concentration Exo III. Thus, the optimal concentration of Exo III is 0.3 U/ $\mu$ L. As shown in Fig. S5B, the value of  $F/F_0$  enhances with the increasing concentration of PvuII from 0.2 to 0.6 U/ $\mu$ L, and reaches a plateau at 0.6 U/ $\mu$ L due to the exhaustion of the demethylated dumbbell probes. Thus, 0.6 U/ $\mu$ L PvuII is used in the subsequent experiments. As shown in Fig. S5C, the value of  $F/F_0$  improves with the increasing concentration of dumbbell probe from 50 to 150 nM, and reaches a plateau at 150 nM. Thus, 150 nM dumbbell probe is used in the subsequent experiments. We further optimized the reaction time. As shown in Fig. S5D, the value of  $F/F_0$  improves with the reaction time from 30 to 60 min, followed by the decrease beyond 60 min.

Thus, the optimal reaction time is 60 min.

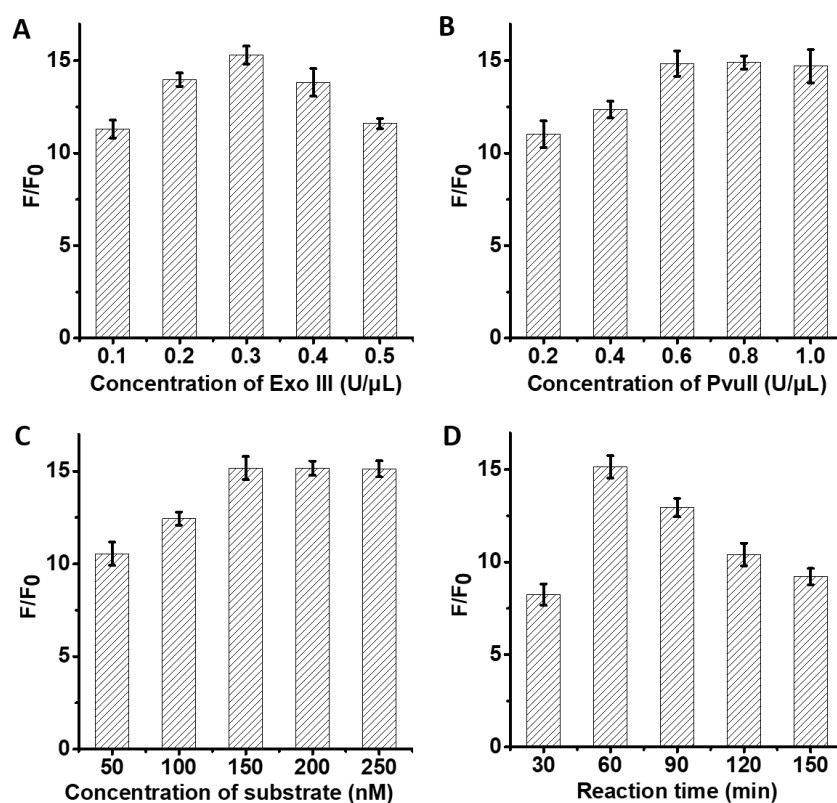


**Fig. S5** (A) Variance of  $F/F_0$  value with different concentrations of Exo III. (B) Variance of  $F/F_0$  value with different concentrations of PvuII. (C) Variance of  $F/F_0$  value with different concentrations of dumbbell probe substrate. (D) Variance of  $F/F_0$  value with reaction time. The MGMT concentration is 10 ng/μL. Error bars represent the standard deviation of three experiments.

### The fluorescence dynamic curves of different MGMT concentrations

We determine the dynamic curve of the reaction system by measuring the variance of Cy5 signal with reaction time (Fig. S6). In the presence of varying concentration of MGMT, the Cy5 signal increases with reaction time from 0 to 120 min (Fig. S6), while no obvious signal enhancement is observed without MGMT (Fig. S6, black line). The results clearly suggest that MGMT can trigger ExoIII-assisted signal amplification for the generation of Cy5 fluorescence.

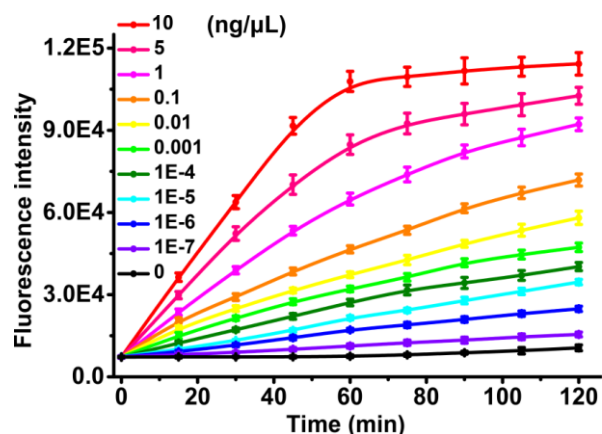


**Fig. S6** Dynamic curve of the reaction system by measuring the variance of Cy5 signal with reaction time.

Error bars represent the standard deviation of three experiments.

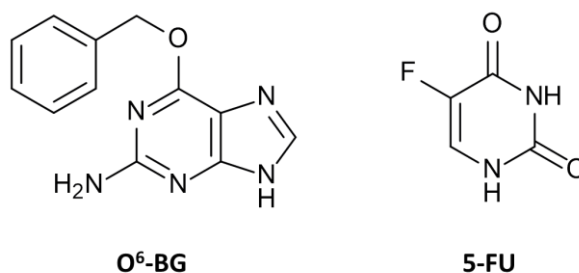


**Fig. S7** Structural formula of O<sup>6</sup>-BG (left) and 5-FU (right).

### Linear equation of ELISA

To determine the expression level of MGMT in cell samples, we measured different concentrations of MGMT using the enzyme-linked immunosorbent assay (ELISA). As shown in Fig. S8, the optical density (OD) at 450 nm shows a linear correlation with the amount of MGMT over a range from  $2.5 \times 10^{-4}$  to  $8.0 \times 10^{-3}$  ng. The regression equation is  $Y = 0.16X + 165.37$  ( $R^2 = 0.997$ ), where  $Y$  is the measured OD and  $X$  is the amount of MGMT.

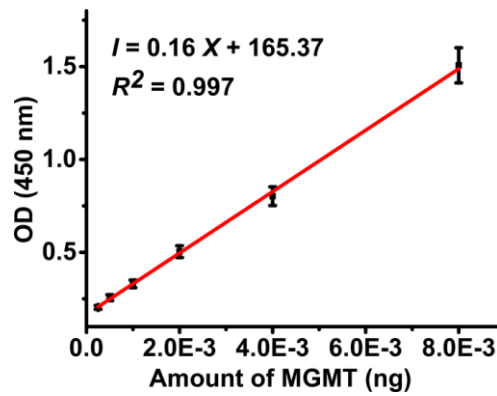


**Fig. S8.** Linear relationship between the optical density (OD) and the amount of MGMT. Error bars represents the standard deviation of three experiments.

### Fluorescence intensity in response to MGMT in different cell lines

We measured the fluorescence intensity generated by MGMT in the nucleus of various cancer cell lines, including human epidermoid carcinoma cells (A431 cells), human cervical cancer cell line (HeLa cells) and human breast cancer cell line (MCF-7 cells). As shown in Fig. S9, a weak fluorescent signal is detected in the control group with the deactivated nucleus extracts (Fig. S9, black column). In contrast, high Cy5 fluorescence signals are generated by HeLa cells ((Fig. S9, green column), MCF-7 cells ((Fig. S9, orange column), and A431 cells (Fig. S9, purple column), suggesting that this method can accurately quantify MGMT activity in different cancer cells.

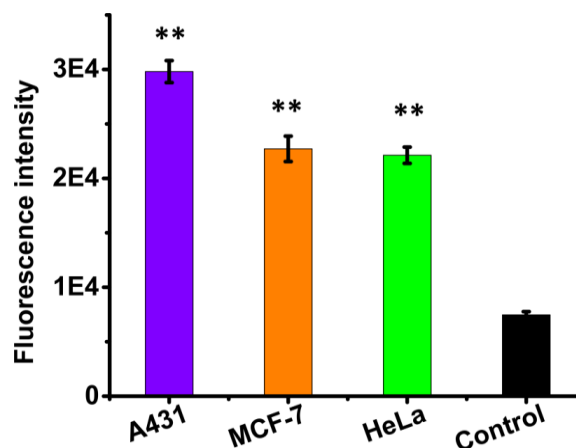


**Fig. S9.** Measurement of Cy5 fluorescence intensity produced by the control group (black column), A431

cells (purple column), MCF-7 cells (orange column), and HeLa cells (green column). The number of each kind of cells is 1000. \* indicates that the fluorescence signals of A431, MCF-7, and HeLa cells nucleus extract are significantly higher than that of control group (\*\* $P < 0.01$ ). Error bars represent the standard deviation of three experiments.

### Correlation of the proposed method with ELISA

We calculated the correlation between the amount of MGMT measured by the proposed method and by ELISA. As shown in Fig. S10, a correlation equation of  $Y = 0.991 X + 0.001$  ( $R^2 = 0.997$ ) is obtained, where  $X$  is the measured MGMT amount by the proposed method and  $Y$  is the measured MGMT amount by ELISA assay. This result clearly demonstrates that the proposed method is in good agreement with ELISA.

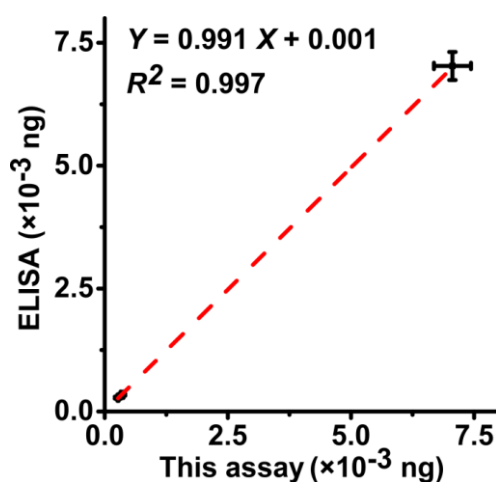


**Fig. S10.** Correlation of the proposed method with ELISA. Analysis of the amount of MGMT from cell samples using ELISA and the proposed method, respectively. Error bars represent the standard deviation of three experiments.

**Table S2.** Recovery studies by spiking MGMT into the diluted human serum (10%).

Sample	Added (U/ $\mu$ L)	Determined (U/ $\mu$ L)	Recovery (%)	RSD (%)
1	$1.0 \times 10^{-2}$	$1.039 \times 10^{-2}$	103.9	3.34
2	$1.0 \times 10^{-5}$	$1.047 \times 10^{-2}$	104.7	2.97
3	$1.0 \times 10^{-7}$	$0.967 \times 10^{-7}$	96.7	3.81

**Table S3.** Comparison of this method with the reported methods for MGMT assay<sup>a</sup>

Strategy	Time (min)	Linear Range	LOD	Real samples	Ref.
Fluorescence switching probes-based assay	Overnight	0–2.5 $\mu$ M	5 nM	living cells	<sup>7</sup>
DNAzyme-based fluorescence sensor	180	0–360 nM	2 nM	living cells	<sup>8</sup>
CRISPR/Cas12a-based cascade signal amplification method	Overnight	10–1000 nM	0.054 nM	living cells	<sup>9</sup>
Graphene oxide-coupled fluorescence assay	120	0.5–35 ng/mL	0.15 ng/mL	10% FBS	<sup>10</sup>
Hairpin probe-based fluorescence assay	180	1–25 ng/mL	0.5 ng/mL	10% FBS	<sup>11</sup>
Exonuclease III-based fluorescence assay	60	$1 \times 10^{-7}$ –0.1 ng/ $\mu$ L	$3.6 \times 10^{-8}$ ng/ $\mu$ L (1.34 fM)	living cells 10% HS	This method

<sup>a</sup> LOD, limit of detection; FBS, fetal bovine serum; HS, human serum.

## References

(1) Fillion, A.; Pinto, J. F.; Granzhan, A. Harnessing an emissive guanine surrogate to design small-molecule fluorescent chemosensors of O-6-methylguanine-DNA-methyltransferase (MGMT). *Org. Biomol. Chem* **2022**,

20, 1888-1892.

(2) Hsu, S. H.; Chen, S. H.; Kuo, C. C.; Chang, J. Y. Ubiquitin-conjugating enzyme E2 B regulates the ubiquitination of O(6)-methylguanine-DNA methyltransferase and BCNU sensitivity in human nasopharyngeal carcinoma cells. *Biochem. Pharmacol.* **2018**, *158*, 327-338.

(3) Xu, Q. F.; Cao, A. P.; Zhang, L. F.; Zhang, C. Y. Rapid and Label-Free Monitoring of Exonuclease III-Assisted Target Recycling Amplification. *Anal. Chem.* **2012**, *84*, 10845-10851.

(4) Yang, Z.; Sismour, A. M.; Benner, S. A. Nucleoside alpha-thiotriphosphates, polymerases and the exonuclease III analysis of oligonucleotides containing phosphorothioate linkages. *Nucleic Acids Res.* **2007**, *35*, 3118-3127.

(5) Cui, L.; Li, Y.; Lu, M.; Tang, B.; Zhang, C.-y. An ultrasensitive electrochemical biosensor for polynucleotide kinase assay based on gold nanoparticle-mediated lambda exonuclease cleavage-induced signal amplification. *Biosens. Bioelectron.* **2018**, *99*, 1-7.

(6) Wang, L.-j.; Zhang, Q.; Tang, B.; Zhang, C.-y. Single-Molecule Detection of Polynucleotide Kinase Based on Phosphorylation-Directed Recovery of Fluorescence Quenched by Au Nanoparticles. *Anal. Chem.* **2017**, *89*, 7255-7261.

(7) Yu, W. T.; Wu, T. W.; Huang, C. L.; Chen, I. C.; Tan, K. T. Protein sensing in living cells by molecular rotor-based fluorescence-switchable chemical probes. *Chem. Sci.* **2016**, *7*, 301-307.

(8) Wang, X. N.; Yi, X.; Huang, Z. M.; He, J. J.; Wu, Z. K.; Chu, X.; Jiang, J. H. "Repaired and Activated" DNase Enables the Monitoring of DNA Alkylation Repair in Live Cells. *Angew. Chem. Int. Ed.* **2021**, *60*, 19889-19896.

(9) Huang, J.; Wang, J.; Wu, Z.; He, J.; Jiang, J.-H. Profiling demethylase activity using epigenetically inactivated DNase. *Biosens. Bioelectron.* **2022**, *207*, 114186.

(10) Le, D. V.; Jiang, J. H. Fluorescence determination of the activity of O-6-methylguanine-DNA methyltransferase based on the activation of restriction endonuclease and the use of graphene oxide.

*Microchimica Acta* **2020**, *187*, 300.

(11) Le, D. V.; Zhou, D. M.; Tang, L. J.; Jiang, J. H.; Yu, R. Q.; Wang, Y. Z. Target-mediated consecutive endonuclease reactions for specific and sensitive homogeneous fluorescence assay of O-6-methylguanine-DNA

methyltransferase. *Anal. Chim. Acta* **2013**, *804*, 252-257.